BJRS

BRAZILIAN JOURNAL
OF
RADIATION SCIENCES
10-03B (2022) 01-13

Analysis of pore geometry in the compacted fine aggregate matrix by x-ray microtomography.

Rogério Ferreira da Costa[a,b,c] and Inaya Corrêa Barbosa Lima[a]

[a]Instituto Alberto Luiz Coimbra de Pós-Graduação e Pesquisa de Engenharia Nuclear da Universidade Federal do Rio de Janeiro, Av. Pedro Calmon, nº 550 - Cidade Universitária, Rio de Janeiro, 21941-594, RJ, Brasil.
[b]Instituto Federal de Educação, Ciência e Tecnologia de Goiás, R.75, nº 46, Centro, Goiânia, 74055-110, GO, Brasil
[c]Universidade Estadual de Goiás, R.14, nº 327 - Jd. América, Morrinhos, 75650-000, GO, Brasil

rogercosta1@hotmail.com,
inaya@coppe.ufrj.br

ABSTRACT

This study employs the X-ray microtomography technique to evaluate the open and closed porosity geometry within fine aggregate matrix (FAM) specimens extracted from different locations of superpave gyratory compactor (SGC) samples compacted with distinct densities. The adoption of advanced techniques such as the X-ray microtomography facilitate the fabrication of FAMs that are more representative of those that comprise asphalt concretes, as well as allow the use of similar replicates in mechanical tests. In addition, the traditional porosity assessment methods are well documented, but provide only global average results for the entire sample. In this context, X-ray microtomography stands out because, besides porosity information, pore distribution and a series of other parameters related to the internal structure of the object can be evaluated. This study evaluated the geometry of open and closed pores of FAM specimens extracted from different locations of SGC compacted samples. From the results and statistical analysis it was observed that there was evidence to conclude that the volumetric density affected the porosity and the number of closed and open pores of the compacted FAM specimens and that the shape of the closed pores is spherical and the shape of the open pores is cylindrical. for SGC samples compressed with 2.26 g/cm^3, 2.34 g/cm^3 and 2.44 g/cm^3.

Keywords: **X-ray microtomography, fine aggregate matrix, pores.**

ISSN: 2319-0612
DOI: https://doi.org/10.15392/2319-0612.2022.1862
Submitted: 2022-01-28
Accepted: 2022-09-21

1. INTRODUCTION

Fine aggregate matrix (FAM) may be used as a predictor of the behavior of asphalt mixtures [1]. The FAM consists primarily of asphalt binder, fine aggregates, fillers and air-filled pores as a major constituent of mixtures [2]. The pores in any structure may or may not be in contact with the material surface. The pores connected to the material surface are usually named as open pores and the pores that are not connected to the surface are called closed pores, even though they are internally connected within the material [3]. The pores that are not connected to the surface are called closed pores, even though they are internally connected within the material [3]. Closed pores can be generated by the sealing process that may occur in the open pores due to the adjustments of the solid phase gases and, consequently, the imprisoned gases may not escape from the structure [4]. Pore size is not precisely defined since its shape is generally irregular and extremely variable. The quantitative pore size description is performed by models of a small number of shapes, such as cylinders, prisms, cavities and windows, slits or spheres [5].

The particles or pores sphericity (sph) has several definitions, among them, the one presented by Mendes [6] which defined it as the relation between surface area and particle volume, numerically; such measurement indicates the similarity of the grain or the pore to a sphere. Rittenhouse determined sph as the relation between the diameter of the circle with an area equal to the projection of the particle and the diameter of the smallest circle circumscribed to the particle, with values ranging from 0 to 1. Briefly, these values range from 0.45 for elongated particles to 0.97 that represent very spherical particles [7].

The tradicional compactation method does not generate a homogeneous distribution of pores within the FAM specimens [8]. Thus, researchers have recently opted for the extraction of small cylindrical specimens from larger samples compacted at the Superpave gyratory compactor (SGC) [1, 9]. This process allows the acquisition of several specimens from a single SGC sample. Reserch indicated that the volumetric characteristics of FAM specimens must be carefully determined to avoid undesired variability in the mechanical behavior of replicates of the same mixture. This also indicates that a certain level of variation can be tolerated around the air void content adopted on the design of FAM without affecting the stiffness of the material [10].

Traditional porosity assessment methods such as mercury porosimetry and Archimedes method are well documented and provide good results for many materials. However, they are only global average results for the entire sample [11]. In this context, X-ray microtomography (μCT.) stands out because, besides porosity information, pore distribution and a series of other parameters related to the internal structure of the object can be evaluated [12]. The study main goal is to evaluate the open and closed pores distribution on FAM specimens extracted from different locations of SGC samples. Statistical analyses are also performed to evaluate the porosity variation and pore number with compactation within the SGC FAM samples. Furthermore, it was possible to determine the open and the closed pores geometric shape of the FAM samples.

2. MATERIALS AND METHODS

The samples were prepared at the Jacques de Medina Geotechnical and Pavement Laboratory located in the Department of Civil Engineering of the Coordination of the Graduate Program in Engineering at the Federal University of Rio de Janeiro (COPPE / UFRJ). The method used to design the FAM samples in this study was recently proposed Amelian *et al*. [13]. This method defines the FAM volumetric characteristics based on the key parameters of the HMA (Hot Mix Asphaltic) mix design. The binder content determined for FAM was 8.49%, while the binder content for the corresponding HMA was 4.90%. The HMA and FAM gradation is shown in Figure 1.

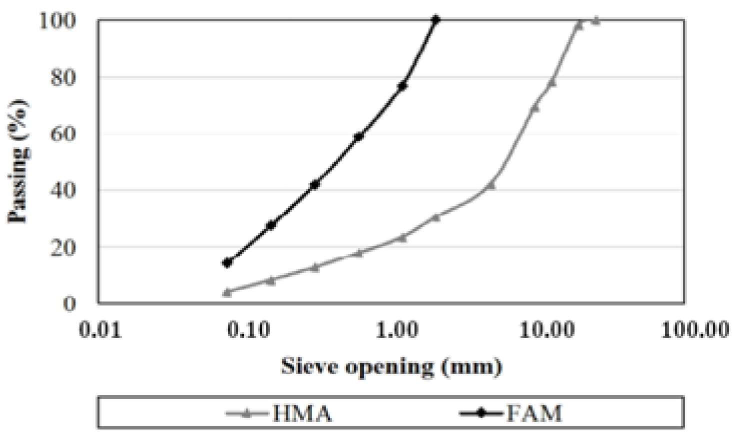

Figure 1 - The HMA and FAM gradation.

The samples FAM1, FAM2 and FAM3 were compacted in the superpave gyratory compactor (SGC) and resulted in the following densities values 2.26 g/cm^3, 2.35 g/cm^3 and 2.44 g/cm^3, respectively, the most compacted samples presented higher density values. Then they were sawn to a final length of approximately 48 mm. Nine specimens from each FAM1, FAM2 and FAM3 were extracted with a cylindrical drill connected to a drilling machine with a diameter of 12 mm in different positions

The image analysis of the specimens of FAMs was performed on the SkyScan model 1173 bench microtomograph (μCT.), installed at X-rays Applied Laboratory on State University of Londrina. It is important to highlight that a threshold value (TH) that separates the two objects included in the ROI must be chosen for the quantification process. There is no default method for determining the value of TH. In this study a global TH value of 30, out of a range from 0 to 255, was selected after a rigorous analysis performed by experienced professionals. After segmentation by global threshoding, the porosity values of the 8 specimens of each FAM1, FAM2 and FAM3 were determined by μCT. at 8 μm resolution. This spatial resolution was chosen because it is the best system resolution to map the small pores of the specimen.

A statistical analysis was performed to identify the possible correlation between the denstity and the porosity at a significance level of 0.05. For that, considering a number of specimens smaller than 30, a t student hypothesis test was carried out to evaluate the dependence among the analyzed variables. The complete dataset data acquired was used to determine the critical t value (Tcrit), which indicates if the density of the specimens affected their porosity, while the t calculated (Tcalc) was defined using the t-distribution [14].

Sph is a measure of how spherical of a 3D object and it was determined through the ratio between the surface area of a sphere (with the same volume as the given particle) to the surface area of the particle [15]. Equation 1 was employed to determined the spherecity [15, 16, 17]:

$$Sph = \frac{\sqrt[3]{\pi}.(6.V)^{2/3}}{A} \tag{1}$$

where V and A are the object volume and surface area respectively

3. RESULTS AND DISCUSSION

As mentioned, the total porosity in any structure is composed of open and closed porosity. Open pores have an external connection, whereas closed pores are isolated within the structure without connection to the surface [3]. The results of open and closed porosity are presented in Figure 2.

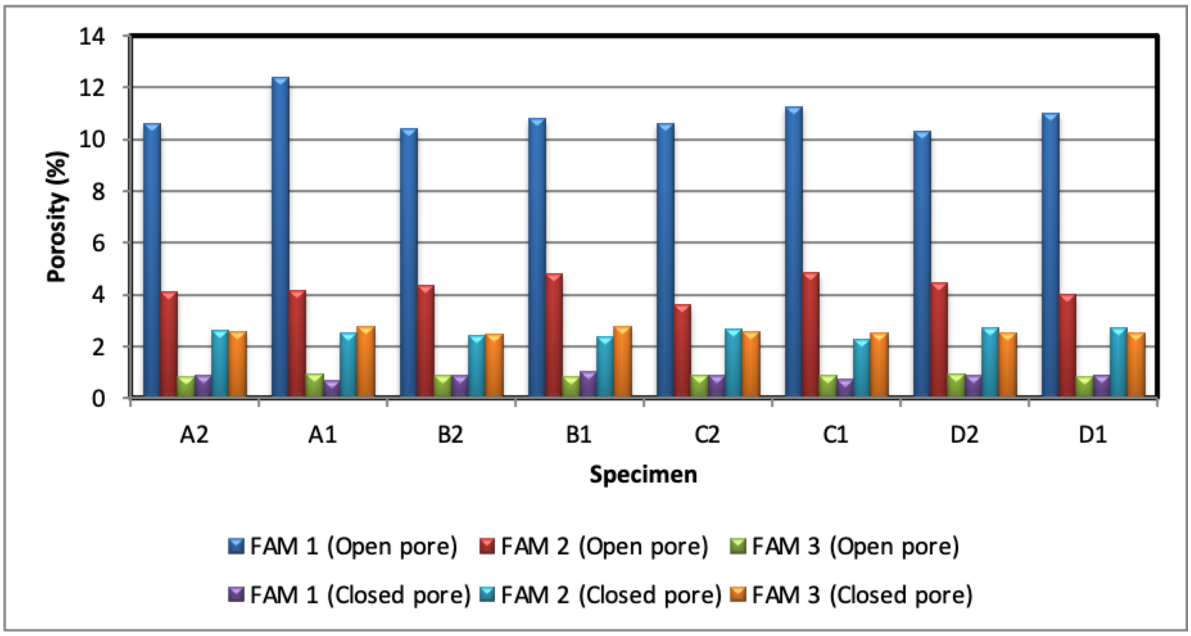

Figure 2 – Open, and closed porosities of the FAM1, FAM2 and FAM3 specimens.

The average porosity shown in Figure 2 for the three compacted FAM1, FAM2 and FAM3, with different densities are 0.85%, 2.53% and 2.58% for closed porosity and 10.81%, 4.30% and 0.89% for open porosity, respectively. The maximum variation observed for the open porosity between the 8 specimens of each FAM in relation to the average was less than 15% and, for closed porosity, the variation did not exceed 10%. In addition, it was observed that the less compacted FAM1 (2.26 g/cm^3) have higher open porosity and lower closed porosity and for the more compacted one (FAM3) the open porosity decreases and the closed porosity increases until it stabilizes when the porosity is approximately 2.3%. In Figure 3 we present the number of open and closed pores for the samples FAM1, FAM2 and FAM3.

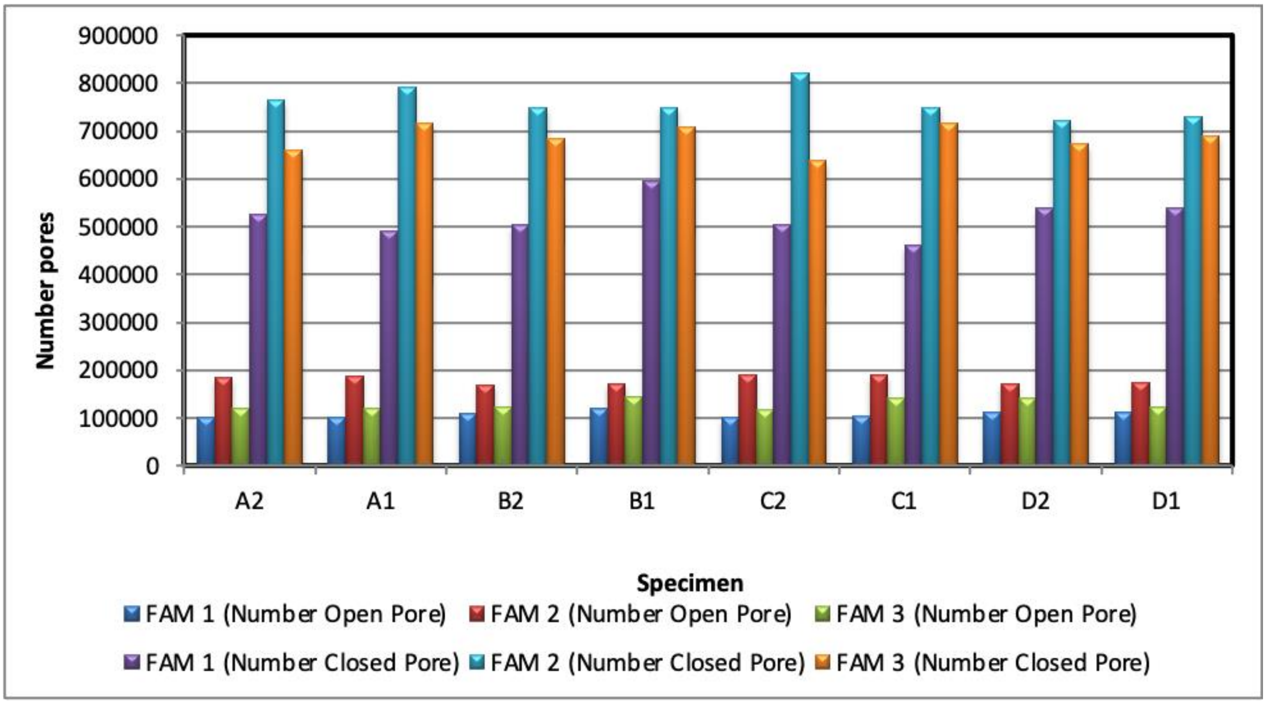

Figure 3 – Number of pores for the samples FAM 1, FAM 2 and FAM 3.

Figure 3 presents the number of open and closed pores of the FAM1, FAM2 and FAM3 samples. It is observed a higher number of pores in FAM2 and this may be related to the fact that when larger pores begin to compress during compaction, they divide into new open and closed pores. For FAM3 previously observed growth behavior was reversed and the number of pores decreased and thus the porosity was reduced. Therefore, the reduction in the total porosity (open porosity + closed porosity) of the FAM2 and FAM3 in relation to the FAM1 is not only related to the variation in the number of pores, since they increase when compared to the less compressed sample.

A Student's t-test statistical analysis was performed to evaluate the experimental hypothesis that a given variation on the amount of volumetric density did affect the porosity and number pores of the samples. Three pairs of specimens were evaluated, that is, FAM1 to FAM2, FAM2 to FAM3, and FM1 to FAM3. In the analysis, a confidence level of 95% was adopted and the T_{crit} value was determined; T_{calc} values taller than the T_{crit} indicate that there is statistical evidence to conclude that the variation on the volumetric density for a given range affected the porosity and number pores of the FAM specimens. table 1 and table 2 summarizes the results obtained for this statistical analysis.

Table 1 - Statistical analysis to evaluate the experimental hypothesis between volumetric densities and closed, open and, total porosity.

FAM range	T_{crit}	$T_{calc\ closed\ porosity}$	$T_{calc\ open\ porosity}$	$T_{calc\ total\ porosity}$
FAM1 to FAM2	2.15	22.87	24.03	21.25
FAM2 to FAM3	2.15	0.7	21.58	28.48
FAM1 to FAM3	2.15	30.74	44.16	40.31

Table 1 showed that there was statistical evidence to conclude that the variation in volumetric density significantly modified the closed, open and total porosity of most FAM specimens, since the T_{calc} is greater than the T_{crit}, so the experimental hypothesis was accepted. Furthermore, these analyzes reinforce the idea that total and open porosity decrease, while closed porosity increases with compaction, with the exception of closed porosity between FAM2 and FAM3, in this case there was no statistically significant difference, since the compaction limit was achieved by the SGC.

Table 2 - Statistical analysis to evaluate the experimental hypothesis between volumetric density and number of closed and open pore.

FAM range	$t_{critical}$	$t_{calc\ to\ number\ closed\ pore}$	$t_{calc\ to\ number\ open\ pore}$
FAM1 to FAM2	2.15	12.27	16.90
FAM2 to FAM3	2.15	4.51	9.62
FAM1 to FAM3	2.15	8.96	4.20

As showed in Table 2, there was statistical evidence to conclude that the variation in volumetric density between specimens affected the number of open and closed pores of the FAM specimens since Tcalc is greater than the t crit, it reinforces the idea that there is really a significant increase in pores in the sample with the compaction in the interval between FAM1 to FAM 2, FAM1 to FAM3 and, a reduction in the number of pores between the interval of FAM2 and FAM3.

The quantities closed porosity (PF), number of closed pores (NPF), total volume of closed pores (VPF) and total area of closed pores (APF) are the means of the nine specimens of FAM 1, FAM 2 and FAM 3 obtained from μCT. These values are useful in determining the mean pore diameter by 3D analysis. These values are shown in table 3.

Table 3 - Quantities for determining the sph of closed pores.

FAM	PF (%)	NPF	VPF (mm^3)	APF (mm^2)
1	0.88	525954	22,83	3184,16
2	2.53	751084	66,37	7434,33
3	2.56	690181	73,78	8229,41

Thus, through the data presented in table 1 and by the equations for the volume and area of the sphere, we found the diameter of the volume (d_V), the diameter of the area (d_A) and then, by the sph equation (1), determined the closed pore shape for each sample. The results are shown in table 4.

Table 4 – Closed pore Sph.

FAM	d_V (μm)	d_A (μm)	Sph
1	43.54	43.86	0.99
2	55.32	56.20	0.97
3	58.90	61.66	0.91

Table 4 showed that the closed pores of the FAMs are spherical, since the Sph of the pores is close to 0.97 [6] in all cases analyzed. In addition, their Sph decreases as the sample is more density. Usually closed pores have a spherical shape. In the FAM 1, FAM 2 and FAM 3, the closed pores are spherical and have average diameters of 43.54 μm, 55.32 μm and 58.90 μm, respectively. It is also observed that the compaction increased the volume of the closed pores. Another important fact is that closed porosity varies with compaction and this cannot be explained only by the increase in the number of closed pores. Thus establishing the ratio of the conversion factor for the closed pore (CF) we have:

$$CF = \left(\frac{NPF_1}{NPF_2}\right) \cdot \left(\frac{{r_1}^3}{r_2^3}\right) \quad (2)$$

Table 5 presents the results of the conversion factor (CF) of the closed porosity of a pair of samples and compares the theoretically obtained value of the closed porosity (PFT) with the experimental value of the closed porosity (PFE) measured by μCT.

Table 5 - FCF result for closed spherical pores

FAM range	PF (%)	CF	PFT (%)	PFE (%)	σ(%)
FAM 1 to FAM 2	0,88	2,93	2,57	2,53	1,1
FAM 1 to FAM 3	0,88	3,25	2,85	2,56	7,6
FAM 2 to FAM 3	2,53	1,11	2,80	2,56	6,3

As the difference σ between PFT and PFE is small for all FAMs, then it is concluded that the theoretical and experimental results are similar and the closed pores can be considered spherical. Obtained from the average of the FAM specimens, the open porosity (PA), number of open pores (NPA), total open pore volume (VPA) and total open pore area (APA) are important values to determine the mean open pore diameter by this method of 3D analysis. These values are found in table 6.

Table 6 - Quantities for determining the sph of open pores.

FAM	PA (%)	NPA	VPA (mm^3)	APA (mm^2)
1	10.81	102606	311,31	20457,08
2	4.31	166260	136,27	11654,09
3	0.88	126900	25,89	3642,18

Thus, through the data in table 4 and then by the sph equation (1), determined the pore shape open for each sample. The results are shown in table 7.

Table 7 – Open pore Sph.

FAM	Sph
1	0.48
2	0.56
3	0.33

Table 7 presents the open pore sph of the samples investigated in this study. The lower sph was 0.33 while the larger value was 0.56. The pores with sph values close to 0.45 should be considered as cylindrical pores [6]. Then, from the results, most of the pore shape is not spherical. As the geometry of the open pore should be alongated then using the equations of volume and area of the cylinder, to calculate the volume diameter (d_V), the area diameter (d_A). The results are shown in table 8.

Table 8 – Diameter and length of open pore.

FAM	d (µm)	l (µm)
1	64	943
2	50	417
3	30	288

Diameters d and lengths l correspond to the elongated cylindrical shaped pores. It is also observed that compaction decreased the volume of open pores (table 8). So the conversion factor for the open pore (FCA) can be written as:

$$CF = \left(\frac{NPA_1}{NPA_2}\right).\left(\frac{r_1^{\,2}.l_1}{r_2^{\,2}.l_2}\right) \tag{3}$$

Table 9 shows the CF results for tube-shaped cylinders that relate the open porosity of a pair of samples and compares the theoretically obtained value of open porosity (PAT) with the experimental value of open porosity (PAE) measured by µCT. As the theoretical and experimental results are similar, open pores can be considered cylindrical.

Table 9- FCA result for cylinders in cylinder shape.

FAM	PA (%)	CF	PAT (%)	PAE (%)	σ(%)
FAM 1 to FAM2	10,81	2,29	4,72	4,31	6,4
FAM 1 to FAM3	10,81	12,05	0,90	0,88	1,6
FAM 2 to FAM3	4,31	5,27	0,82	0,88	5,0

As the difference σ between PAT and PAE is small for all FAMs, then it is concluded that the theoretical and experimental results are similar and the open pores can be considered cylindrical.

4. CONCLUSIONS

This study evaluated the distribution of open and closed pores of FAM specimens extracted from different locations of SGC compacted samples. From the results and analyses, it could be observed that the specimens extracted showed that there was statistical evidence to conclude that the volumetric density affected the porosity and the number of closed and open pores of the compacted FAM specimens with a significance level of 95%. Furthermore, it was found that the open porosity decreases, while the closed porosity increases for all analyzed intervals, with the exception of closed porosity between FAM2 and FAM3, in this case there was no statistically significant difference. The number of closed and open pores increases between the range of FAM1 and FAM2 and decreases between FAM2 and FAM3. The shape of the closed pores is spherical and the shape of the open pores is cylindrical for the SGC samples packed with 2.26 g/cm^3, 2.34 g/cm^3 and 2.44 g/cm^3.

ACKNOWLEDGMENTS

The authors thanks the Brazilian agencies CNPq (National Council for Scientific and Technological Development) for financial support, the Laboratory of Applied Nuclear Physics – Department of Physics, State University of Londrina and Laboratory of Applied Phys to Biomed and Environmental Sci/State University of Rio de Janeiro for help during image acquisition and reconstruction.

REFERENCES

[1] ARAGÃO, F. T. S.; VARGAS, G. A. B.; HARTMANN, D.A.; OLIVEIRA, A.D.; KIM, Y. R. Characterization of Temperature- and Rate-Dependent Fracture Properties of Fine Aggregate Bituminous Mixtures Using an Integrated Numerical-Experimental Approach. **Engineering Fracture Mechanics,** v. 180, p. 195 – 212, 2017.

[2] KIM, Y. R. ; LITTLE, D. N. ; SONG, I. Effect of Mineral Fillers on Fatigue Resistance and Fundamental Material Characteristics: Mechanistic Evaluation. **Transportation Research Record: Journal of the Transportation Research Board,** v.1832, p. 1 – 8, 2003.

[3] KLOBES, P.; MEYER, K.; MUNRO, R. G. **Porosity and specific surface area measurements for solid materials.** National Institute of Standards and Technology, Washington, 2006.

[4]RICHERSON, D. W. **Modern Ceramic Engineering: Properties, Processing and Use in Design**, 3rd ed. Marcel Dekker, New York, 2006.

[5] ROUQUEIROL J.; AVNIR D.; FAIRBRIDGE C. W.; EVERETT D. H.; HAYNES J. H.; PERNICONE N. ; RAMSAY J. D. F. ; SING K. S. W. ; UNGER K. K. Recommendations for the characterization of porous solids, **Pure & Appl. Chern.**, v. 66, pp. 1739-1758, 1994.

[6] MENDES, J. C**. Stratigraphy and sedimentology: structural geology and aerophotogeology**. National Book Institute, Brasília, 1972.

[7] RITTENHOUSE, G. A visual method of estimating two-dimensional sphericity. **J Sedim Petrol**., v. 13, p. 79-81, 1943.

[8] ZOLLINGER, C. J. Application of Surface Energy Measurements to Evaluate Moisture Susceptibility of Asphalt and Aggregates. Master's thesis. Texas A&M University, College Station, 2005.

[9] ARAGÃO, F. T. S.; HARTMANN, D. A.; KIM, Y. R.; MOTTA, L. M. G.; HAFT-JAVAHERIAN, M. Numerical-Experimental Approach to Characterize Fracture Properties of Asphalt Mixtures at Low In-Service Temperatures. **Transportation Research Record: Journal of the Transportation Research Board**, v. 2447, p. 42-50, 2014.

[10] OSMARI, P. H.; COSTA, R. F.; ARAGÃO, F. T. S.; BRAZ, D.; BARROSO, R. C.; NOGUEIRA, L. P.; NG, A. K. Y. Determination of Volumetric Characteristics of FAM Mixtures using X-Ray Micro-Computed Tomography and Their Effects on the Rheological Behavior of the Material. **Transportation Research Record: Journal of the Transportation Research Board**, v. 2674, p. 97–107, 2020.

[11] PESSOA, J. R. C.; DOMIGUEZ, J. S.; CARVALHO, G.; ASSIS, J. T. Concrete porosity determined by X-ray microtomography and image processing. **ABPE**, v. 14, p. 20-26, 2014.

[12] GOPALAKRISHNAN, K.; CEYLAN, H.; INANC, F. Using X-ray computed tomography to study paving materials. **Construction Materials**, v. 160, p. 15-23, 2007.

[13] AMELIAN, S.; KIM, Y. R.; OSMARI, P. H.; ARAGÃO, F. T. S.; BRAZ, D. Development of a Volumetric Mix Design Approach for Fine Aggregate Matrix (FAM) and Validation with

Micro-CT Method, In: **TRANSPORTATION RESEARCH BOARD**, 2019, Annals Washington, D. C., USA, p. 1-8.

[14] GRAVETTER, F. J.; WALLNAU, L. B., 1995, Statistics for the behavioral sciences. 2 ed. St.Paul, West Publishing, p.429.

[15] CTAnalyser. **The User's Guide, Skyscan/Bruker micro-CT, Kartuizerweg 3B 2550 Kontich**, Belgium, 2012.

[16] WADEL, H., Volume, shape and roundness scale for sedimentary rock particles, **Journal of Geology**, v. 40, pp. 443-451, 1932.

[17] PINTO, T. C. S. ; LIMA, O. A.. ; FILHO, L. S. L. Sphericity of apatite particles determined by gas permeability through packed beds. **Mining, Metallurgy & Exploration**, v. 26, pp. 105 – 108, 2009.